International Journal of GEOMATE, Aug. 2019, Vol.17, Issue 60, pp.1- 8
Geotec., Const. Mat. & Env., DOI: https://doi.org/10.21660/2019.60.19289
ISSN: 2186-2982 (Print), 2186-2990 (Online), Japan

LOCAL SCOURING AROUND PILE AND CURVED CHANNEL

*Dantje K. Natakusumah[1], Dhemi Harlan[1], and Sony Herdiansyah[2]

[1]Faculty of Civil and Environmental Engineering, Institut Teknologi Bandung, Indonesia
[2]Post Graduate Alumni of Civil Engineering Department, Institut Teknologi Bandung, Indonesia

*Corresponding Author, Received: 21 Dec. 2018, Revised: 25 Jan. 2019, Accepted: 12 Feb. 2019

ABSTRACT: One of the destructive water force is scouring due to obstruction or alteration of its flow. Understanding the process is crucially necessary to be able to predict and anticipate scouring. FVCOM model is used in this study to simulate scouring on the pile and curved channel. FVCOM model calibrated with a previous experimental study on straight channel case, modeled curved channel to reveal its capability to capture secondary flow phenomenon, and modeled flow with a pile on a curved channel to reveal its pattern. This study is intended to reveal the scouring pattern on the pile and curved channel. FVCOM model is based on the finite volume method to solve Navier Stokes hydrodynamics, Meyer Peter Muller sediment transports, and Exner bed updates equations. FVCOM model has successfully captured flow behavior around the pile and curved channels such as downflow on upstream of the pile, wake vortex on downstream of the pile, and secondary flow on the curved channel. Pile and curved channel caused scouring in each case. Together, they make a scouring phenomenon even more. This is well proven in FVCOM simulation as the pile on curved channel scoured deeper compared to those on straight one.

Keywords: Scouring, FVCOM, Pile, Curved channel

1. INTRODUCTION

Water has numerous benefits for human life but also has the potential to damage people's lives. Human as a water user should be able to predict and anticipate its potential destructive force.

One of the destructive water forces is scouring due to obstruction or alteration of its flow, such as pile. Understanding the process is crucially necessary to be able to predict and anticipate scouring. The numerical model is one of the approaches to predict water flow and scouring behavior.

Real world situation often faced with the condition that pile should be built on a curved channel or river. Because of that, studies on this problem is necessary to be conducted.

FVCOM numerical model is used in this study to simulate scouring on the pile and curved channel. The numerical model is selected on this study because of its lower cost and modeling time, and nowadays computer resources that capable to simulate complex flow phenomenon. This study is intended to reveal the scouring pattern on the pile and curved channel.

2. LITERATURE REVIEW

2.1 Fluid Characteristic

Although the differences in fluid and solid objects can be explained qualitatively based on its molecular structure, a more specific difference is based on how the fluids and solids deform due to external forces. The fluid is defined as a substance that continually deforms (flows) when it is given shear force. Although solids also can deform (value of the deformation is very small), a solid object deformation is not continuous (no flow) [1].

Munson et al. [1] explained that laws that apply in the fluid are Newton's laws of motion, conservation of mass, and the first and second laws of thermodynamics. Thus, there are similarities between the approaches used in the analysis of fluid motion with the approach used in solid objects.

2.2 Scouring and Sediment Transport

Annandale [2] defines scour as an excessive erosion event at a particular location. Erosion is transported sediment material event due to specific flow phenomena, such as deflection of flow around the bridge pile, narrowing flow at bridge abutments, supercritical flow from dam spillway, and so forth. The information necessary to analyze the phenomenon of scours includes sediment ability to resist, sediment transport capacity of flowing water, and critical value associated with sediment transport capacity when sediment begins to move, known as incipient motion criteria.

Incipient motion occurs when the value of sediment transport capacity due to water flow just exceeds the value of sediment ability to resist erosion. This event is the beginning of erosion and will continue until a new equilibrium is reached. A new equilibrium is a state where the sediment transport capacity due to the flow of water becomes equal to or lower than sediment ability to resist erosion. In such that condition, maximum scouring is reached.

Quantification of the value of sediment transport is not an easy task. In general, the approach of using flow indicators or parameters with ties or influence on sediment transport is employed. Indicators or parameters used such as shear stress, average velocity, and stream power. The methods used to quantify the amount or value of sediment transport has very high variability and inconsistent yield trends. This causes practical problems for researchers and practitioners to analyze the scour phenomenon. To deal with this problem, the numerical model of sediment transport should be conducted carefully, often calibrated to experimental study or analytical one.

2.3 Numerical Methods

Numerical modeling of water flow phenomena is an analysis of the water flow system and process based on computer simulations. Versteeg and Malalasekara [3] describes the use of numerical methods several advantages compared to the experimental approach in the case of a fluid system, including:

- Lower cost and modeling time.
- Capability to simulate the system where controlled experiments are difficult or impossible to implement (e.g., very large systems).
- Ability to model the system with a high level of danger or outside the limits that can be retained by the system (for example, is the study of security and disaster scenario).
- Unlimited levels of results details.

A numerical model is an algorithm calculation performed by the computer with the input or the input specified by the user. Numerical modeling is generally divided into three processes, namely pre-processor, solver and post-processor.

Pre-processor is input from water flow problems into numerical model consists of: definition of model domain, division of domain into small parts with simple geometry that do not overlap (also called a grid, mesh, cell, or element), the selection and discretization governing equation that describes the phenomenon of water flow, determining or defining property of water flow, and selection of flow boundary conditions that can represent actual water flow in reality.

There are three main techniques or methods to solve governing equations that describe the phenomenon of water flow, finite difference method; finite volume method; and finite element method.

Post-processor is the extraction process output, visualization of flow parameters, and interpretation of modeling results. Many computer applications can facilitate the extraction process and visualization of modeling output. Visualization can be done by displaying an animated and dynamic result on the computer screen.

2.4 Finite Volume Method

Mazumder [4] states that in the finite volume method, governing equations in the form of partial derivative equations solved at each volume control. The first step is to divide the computational domain into cells, as can be seen in Figure 1. Cells have a simple shape and can be sized differently from one another. Boundary line between two cells known as cell surface. Points within cells called nodal. Flow parameters information is stored in each cell, called the center of the cell. In Figure 1, the cell center is a small box that is contained in the triangular cell, whereas the nodal point is thick at both ends of the line that limits one cell to another.

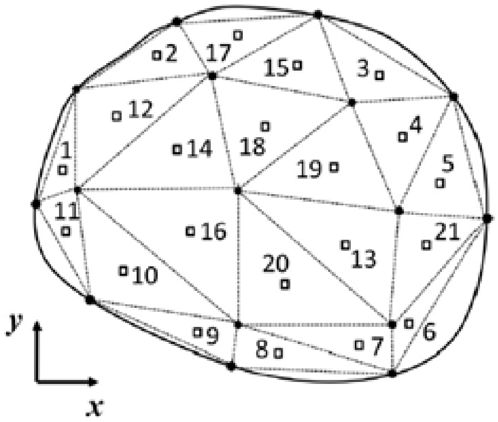

Fig. 1 A schematic representation of the domain and mesh infinite volume method.

Unlike the finite difference method, in the finite volume method, the equation is not immediately resolved, but integrated into each cell in the computational domain then approximation and completion are made. Because there are no cells outside the domain boundary, the boundary conditions cannot be directly resolved.

The most important property in the finite volume method is called conservation property. The amount of variable transfer rate per unit area of the cell surface called a flux. In the case of diffusion, the amount of flux is proportional to the gradient of variable magnitude being simulated.

Fundamentally, the finite volume method is a flux balance equation. Thus, conservation characteristic is always automatically maintained in a finite volume method.

2.5 FVCOM Model

FVCOM is a 3-D model of primitive equations for free surface flow simulation with a finite volume approach on irregular grid developed by Chen and Beardsley [5]. FVCOM model has been equipped with a sediment calculation module refers to the ROMS model consisting of suspended sediment and bed sediment transport. ROMS is a model of sediment transport with a structured grid which is then modified to accommodate irregular grid (unstructured) on the FVCOM model.

In the FVCOM finite volume method, a triangular mesh is applied with an irregular grid. Each element consists of three nodes, one centroid, and three sides. Size of mesh formed in the domain is defined by the user. To improve the accuracy of computational results, vector variables of u and v (velocity in the direction of x and y) placed at elements centroid (center point), while scalar variables are placed at nodal points.

2.6 Local Scour around Bridge Pile

Local scour bed scouring that occurs locally around the buildings or obstructions in a stream of water. Due to the buildings or other obstructions, the flow was interrupted, and the flow parameters were changed.

Adikesuma [6] states that basic mechanisms that cause scours are a vortex that occurs at the bed, known as Horseshoe Vortex. Ameson et al. [7] give a schematic representation of the dimensions of the phenomenon of Horseshoe Vortex at bridge piers as can be seen in Figure 2 and Figure 3.

Whirlpool also occurs in downstream of building or barrier is known as Wake Vortex as can be seen in the illustration in Figure 3. The intensity of Wake Vortex quickly diminished with increasing distance downstream of buildings or obstructions. This then leads to the disposition of the base material on the downstream structure.

3. GOVERNING EQUATION AND DISCRETIZATION

3.1 Hydrodynamic Equations

By ignoring the Coriolis parameter and non-hydrostatic pressure, the governing equations used in the FVCOM model is the continuity and momentum equation as follows:

$$\frac{\partial u}{\partial t}+u\frac{\partial u}{\partial x}+v\frac{\partial u}{\partial y}+w\frac{\partial u}{\partial z}=-\frac{1}{\rho_0}\frac{\partial P}{\partial x}+\frac{\partial}{\partial z}\left(K_m\frac{\partial u}{\partial z}\right)+F_u \quad (1)$$

$$\frac{\partial v}{\partial t}+u\frac{\partial v}{\partial x}+v\frac{\partial v}{\partial y}+w\frac{\partial v}{\partial z}=-\frac{1}{\rho_0}\frac{\partial P}{\partial y}+\frac{\partial}{\partial z}\left(K_m\frac{\partial v}{\partial z}\right)+F_v \quad (2)$$

$$\frac{\partial w}{\partial t}+u\frac{\partial w}{\partial x}+v\frac{\partial w}{\partial y}+w\frac{\partial w}{\partial z}=\frac{\partial}{\partial z}\left(K_m\frac{\partial w}{\partial z}\right) \quad (3)$$

$$\frac{\partial u}{\partial x}+\frac{\partial v}{\partial y}+\frac{\partial w}{\partial z}=0 \quad (4)$$

Equations (1)-(3) is momentum equations and eq. (4) Is continuity equation where x, y, and z are the Cartesian coordinate system, while u, v, and w are the components of velocity in directions of x, y, and z, ρ is density of water, P is hydrostatic pressure, g is gravitational acceleration, K_m is vertical component of Eddy viscosity, and F_u, F_v represents horizontal force. Illustration of an orthogonal coordinate by Chen et al. [8] can be seen in Figure 4, where the total water column is calculated using Eq. (5), H is bed elevation relative to z = 0, and ζ is the elevation of free surface water relative to z = 0.

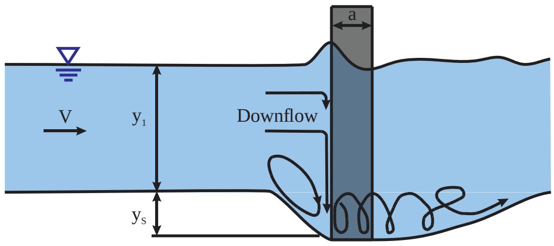

Fig. 2 Two-dimensional sketch of Horseshoe Vortex phenomena on bridge pile (Ameson et al., 2012).

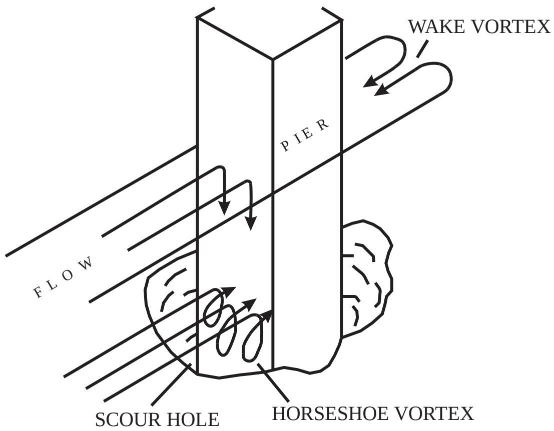

Fig. 3 Three-dimensional sketch of Horseshoe Vortex phenomenon at bridge pile (Ameson et al., 2012).

$$D=H+\zeta \quad (5)$$

where $p = p_a + p_H + q$ and p_H meet the following conditions:

$$\frac{\partial p_H}{\partial z}=-\rho g \rightarrow p_H=\rho_0 g+g\int_z^0 \rho\, dz' \quad (6)$$

Values of u, v, and w parameters on surface and bottom boundary condition at the absence of evaporation, transpiration and bottom fluxes can be seen as in Eqs. (7) and (8).

$$w = \frac{\partial \zeta}{\partial t} + u\frac{\partial \zeta}{\partial x} + v\frac{\partial \zeta}{\partial y}\ at\ z = \zeta(x,y,t) \quad (7)$$

$$w = -u\frac{\partial H}{\partial x} - v\frac{\partial H}{\partial y}\ at\ z = -H(x,y) \quad (8)$$

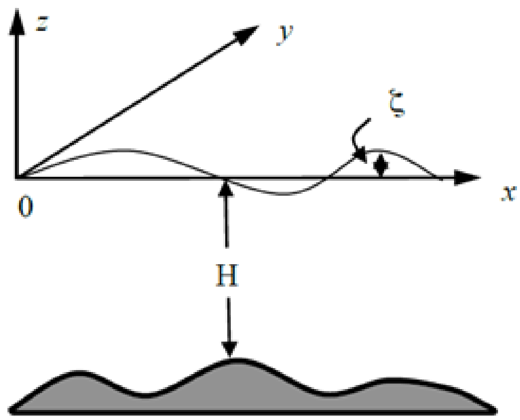

Fig. 4 Illustration of the orthogonal coordinate used in the FVCOM model (Chen et al., 2013).

To solve the problems of irregular bathymetry, use the coordinates of sigma (σ) as defined as:

$$\sigma = \frac{z-\zeta}{D} \quad (9)$$

Due to the σ price that varies from 0 (on the surface) to -1 (at the bottom), then, Eqs. (1)-(4) turn out to be as follows:

$$\frac{\partial uD}{\partial t} + \frac{\partial u^2 D}{\partial x} + \frac{\partial uvD}{\partial y} + \frac{\partial u\omega}{\partial \sigma} = -gD\frac{\partial \zeta}{\partial x} - \frac{gD}{\rho_0}\left[\frac{\partial}{\partial x}\left(D\int_\sigma^0 \rho\, d\sigma'\right) + \sigma\rho\frac{\partial D}{\partial x}\right] + \frac{1}{D}\frac{\partial}{\partial \sigma}\left(K_m\frac{\partial u}{\partial \sigma}\right) + DF_x \quad (10)$$

$$\frac{\partial vD}{\partial t} + \frac{\partial uvD}{\partial x} + \frac{\partial v^2 D}{\partial y} + \frac{\partial v\omega}{\partial \sigma} = -gD\frac{\partial \zeta}{\partial y} - \frac{gD}{\rho_0}\left[\frac{\partial}{\partial y}\left(D\int_\sigma^0 \rho\, d\sigma'\right) + \sigma\rho\frac{\partial D}{\partial y}\right] + \frac{1}{D}\frac{\partial}{\partial \sigma}\left(K_m\frac{\partial v}{\partial \sigma}\right) + DF_y \quad (11)$$

$$\frac{\partial wD}{\partial t} + \frac{\partial uwD}{\partial x} + \frac{\partial vwD}{\partial y} + \frac{\partial w\omega}{\partial \sigma} = -\frac{1}{D}\frac{\partial}{\partial \sigma}\left(K_m\frac{\partial w}{\partial \sigma}\right) \quad (12)$$

$$\frac{\partial \zeta}{\partial t} + \frac{\partial Du}{\partial x} + \frac{\partial Dv}{\partial y} + \frac{\partial \omega}{\partial \sigma} = 0 \quad (13)$$

where DF_X and DF_Y is defined as follows

$$D\tilde{F}_x = \frac{\partial}{\partial x}\left[2\overline{A_m}H\frac{\partial \bar{u}}{\partial x}\right] + \frac{\partial}{\partial y}\left[\overline{A_m}H\left(\frac{\partial \bar{u}}{\partial y} + \frac{\partial \bar{v}}{\partial x}\right)\right] \quad (14)$$

$$D\tilde{F}_y = \frac{\partial}{\partial x}\left[\overline{A_m}H\left(\frac{\partial \bar{u}}{\partial y} + \frac{\partial \bar{v}}{\partial x}\right)\right] + \frac{\partial}{\partial y}\left[2\overline{A_m}H\frac{\partial \bar{u}}{\partial x}\right] \quad (15)$$

3.2 Turbulent Term Closure

Primitive equations described in sub-section 3.1 still require horizontal and vertical diffusion values to be resolved. Smagorinsky eddy parameterization methods used in the FVCOM model for horizontal diffusion as can be seen in the following equation:

$$A_m = 0.5C\Omega^u\sqrt{\left(\frac{\partial u}{\partial x}\right)^2 + 0.5\left(\frac{\partial u}{\partial x} + \frac{\partial u}{\partial y}\right)^2 + \left(\frac{\partial v}{\partial y}\right)^2} \quad (16)$$

Where C is a constant parameter, and Ω^u is the area of the momentum control element. A_m value varies depending on model resolution and the horizontal velocity gradient. A_m value decreases as the grid size or horizontal velocity gradient decreases?

3.3 Scouring and Sediment Transport Equation

FVCOM model has been equipped with the module to calculate suspended sediment and bed sediment transport, and there are areas near the bed where there is no clear distinction between these two sources. On implementation, suspended sediment and suspended sediment are calculated separately and added together to produce total sediment transport.

3.3.1 Suspended sediment transport equation

Suspended sediment model use the concentration approach with the following evolution equation:

$$\frac{\partial C_i}{\partial t} + \frac{\partial uC_i}{\partial x} + \frac{\partial vC_i}{\partial y} + \frac{\partial (w-w_i)C_i}{\partial x} = \frac{\partial}{\partial x}\left(A_h\frac{\partial C_i}{\partial x}\right) + \frac{\partial}{\partial y}\left(A_h\frac{\partial C_i}{\partial y}\right) + \frac{\partial}{\partial z}\left(K_h\frac{\partial C_i}{\partial z}\right) \quad (17)$$

Where C_i is sediment concentration I, A_h is horizontal eddy viscosity, K_h is vertical eddy viscosity, and w_i is the settling velocity. On the surface, there is a no-flux boundary condition, while at the bottom, sediment flux is the difference between the deposition and erosion. Both of these boundary conditions are mathematically presented in Eqs. (18) And (19). The rate of erosion is calculated using Eq. (20).

$$K_h\frac{\partial C_i}{\partial z} = 0\ at\ z = \zeta \quad (18)$$

$$K_h\frac{\partial C_i}{\partial z} = E_i - D_i\ at\ z = -H \quad (19)$$

$$E_i = \Delta t\ Q_i(1-P_b)F_{bi}\left(\frac{\tau_b}{\tau_{ci}} - 1\right) \quad (20)$$

where Q_i is the erosive fluxes, P_b is the porosity of sediments, and τ_{ci} are critical shear stress of sediment i.

Sediment eroded when the local shear stress that occurs is greater than critical shear stress. Balanced advection, vertical diffusion, sediments transported and deposited sediment will generate a sediment concentration profile. Settling term (4th term in the evolution equation sediment concentration) need to be considered with caution because there is a sharp profile of concentration gradient near the base. FVCOM model used a flux-limited scheme. This scheme used a min-mod limiter and eliminated second-order accuracy in extreme gradients. Settling flux on the bed is stored as a deposition flux in the Eq. (19).

3.3.2 Bed sediment transport and morphology equations

To calculate the thickness of eroded sediment, the Exner mass balance equation is used, such as the following:

$$\frac{\partial \eta}{\partial t} = -\frac{1}{\varepsilon_0}\nabla \cdot q_s \tag{21}$$

Where η is a bottom elevation, t is time, ε_0 is porosity, and ∇q_s is bed sediment flux gradient in space.

Sediment flux is computed by using Meyer-Peter and Muller scheme. In this scheme, the sediment flux is calculated based on the difference of actual stress with critical stress, such as the following:

$$q_{s^*} = K_{MPM}(\tau_{*sk} - \tau_{*c})^{3/2} \tag{22}$$

Where q_{s*} is a flux of sediment, K_{MPM} is an empirical correction factor (K_{MPM} = 8 in the experiment Meyer-Peter and Muller), τ_{*sk} is shear stress at the bed, and τ_{*c} is critical shear stress. In this equation, the asterisk stating that the variable is dimensionless. To get the value of dimensionless variables, use the following equation:

$$q_{s^*} = \frac{q_s}{[(s-1)gD^3]^{1/2}} \tag{23}$$

$$\tau_* = \frac{u^2}{(s-1)gD} \tag{24}$$

where q_s is volumetric sediment discharge per unit width, u_* is shear velocity, s is a specific weight of sediment, g is gravitational acceleration, D is water depth.

3.4 Finite Volume Discretization

Similar to the finite element method, the numerical computation domain is divided into several horizontal triangle cells. Cells triangle consists of three nodes, one centroid, and three sides (Figure 5).

Integration of equation (13) to the area of triangular cells provide:

$$\iint \frac{\partial \zeta}{\partial t} dx\, dy = \iint \left[\frac{\partial (uD)}{\partial x} + \frac{\partial (vD)}{\partial x}\right] dx\, dy =$$

$$\oint v_n D\, ds' \tag{25}$$

where i_n is the velocity component normal to the cell edge and s is three sides of a triangle.

Equation (25) are integrated numerically by the 4th order Runge-Kutta scheme, with the following procedures:

$$\zeta_j^0 = \zeta_j^n \tag{26}$$

$$R_\zeta^0 = R_\zeta^n = \sum_{m=1}^{NT(j)}[(\Delta x_{2m-1} v_m^n - \Delta y_{2m-1} u_m^n) D_{2m-1}^n + (\Delta x_{2m} v_m^n - \Delta y_{2m} u_m^n) D_{2m}^n] \tag{27}$$

$$\zeta_j^k = \zeta_j^0 - a^k \frac{\Delta t R_\zeta^{k-1}}{2\Omega_j^\zeta} \tag{28}$$

$$\zeta_j^{n+1} = \zeta_j^n \tag{29}$$

where k = 1, 2, 3, 4 and (α1, α2, α3, α4) = (1/4, 1/3, 1/2, 1). N represents n-th time-step. Ω is area bounded by the midpoint of the side of a triangle around the nodal point.

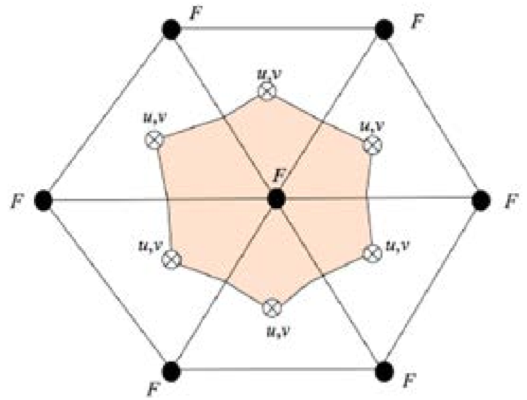

Fig. 5 Triangles cell illustration and variables location (Chen et al., 2013).

With the same way integration, momentum equations and sediment transport can be discretized using a finite volume scheme. Space discretization is based on flux balance on each cell, and time discretization using the 4th order Runge-Kutta method.

4. RESULT AND DISCUSSION

4.1 Pile on Straight Channel

The domain is 6 meters long and 1.1 meters wide. 10 cm x 10 cm rectangle pile is placed right in the middle. Water flows at the constant discharge of 52 L/s with 22 cm water depth and initial bed sediment thickness of 15 cm.

Simulation results show that bed roughness value affected the rate and maximum scour that occurred around a bridge pile — the greater the value of bed roughness, the greater and faster the scouring that occurs.

Figure 6-7 shows current velocity vectors and magnitudes on vertical cross-section upstream of the bridge pile using the FVCOM model. Figure 8-9 shows current velocity vectors and magnitudes on the horizontal cross section around a bridge pile using the FVCOM model.

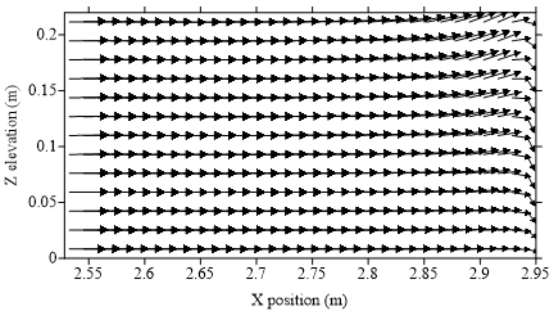

Fig. 6 Velocity vector on the upstream of the pile (FVCOM).

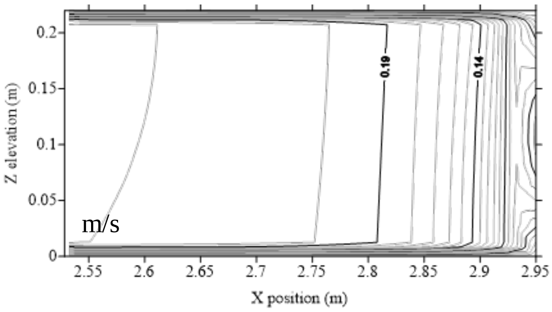

Fig. 7 The magnitude of the velocity vector on the upstream of the pile (FVCOM).

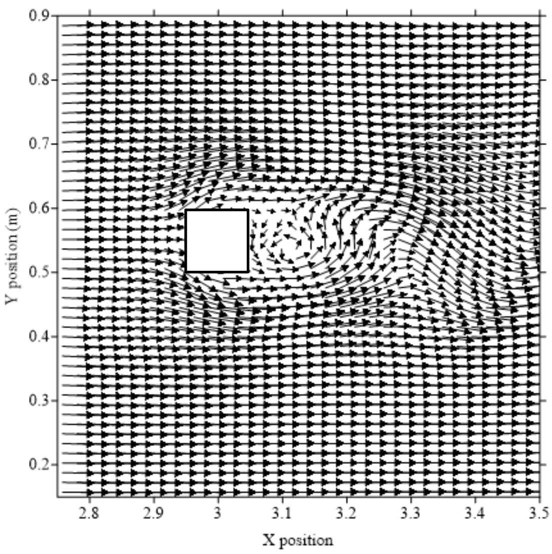

Fig. 8 Horizontal vortex velocity vector around the pile on the middle layer (FVCOM).

Figure 6 and 7 show that FVCOM model simulation failed to capture vertical vortex phenomenon on upstream of the pile compared to a model of Thanh et al. [9] in Fig. 8, this is caused by the velocity vector of the vertical direction is a

The result of the movement of the axis of sigma and not

the actual vertical direction movement. Even though, FVCOM model simulation can capture horizontal vortex phenomena (wake vortex) on downstream of the pile very well, as can be seen in Figs. 9 and 10.

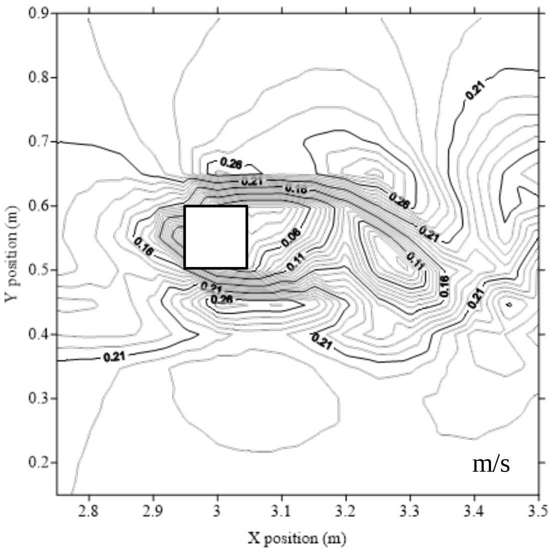

Fig. 9 Magnitude of the horizontal vortex velocity vector around the pile on the middle layer (FVCOM).

Scouring that occurs in the FVCOM model simulation along with comparisons with experimental and FSUM model simulation conducted by Thanh et al. [9] presented in a time-series graph which can be seen in Fig. 11.

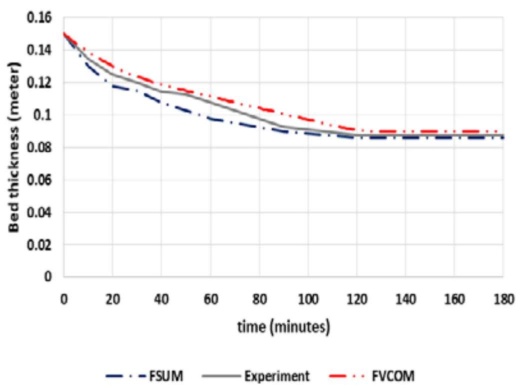

Fig. 11 Time-series thickness of sediments due to scour around bridge pile.

Pearson correlation value and the error rate of FVCOM model results compared with the results of experimental studies by Thanh et al. [9]. Correlation value and the error rate is then compared with a correlation value and the error rate resulted by FSUM numerical modeling by Thanh et al. [9]. These values can be seen in Table 1.

Table 1 Comparison of FVCOM and FSUM results

Model	Pearson correlation	Error (%)
FSUM	0.98	6.82
FVCOM	0.99	5.96

4.2 Curved Channel

In this curved channel case, the model domain is a hypothetical 180^0 curved channel with 200m wide. The slope is set to be 0.0002. Upstream and downstream boundary is constant 2m water depth. Model domain is shown in Fig. 12. Water flows from the upper left boundary to the lower left boundary.

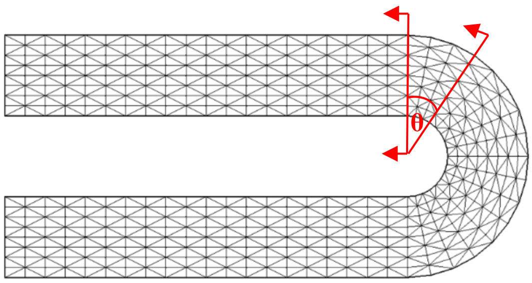

Fig. 12 Domain and 2D Mesh of curved channel

Model results shown in this section is the velocity vector of secondary flow on the cross-section along a curved channel as illustrated in Fig. 12 and can be seen in Fig. 13-15. From those results, FVCOM simulated secondary flow on a curved channel very well.

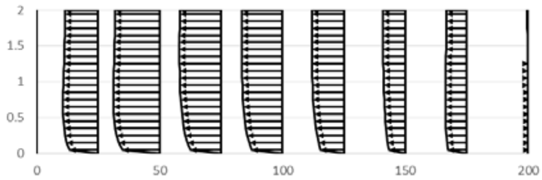

Fig. 13 Velocity vector on $\theta = 0^0$

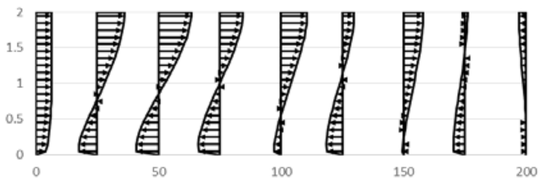

Fig. 14 Velocity vector on $\theta = 45^0$

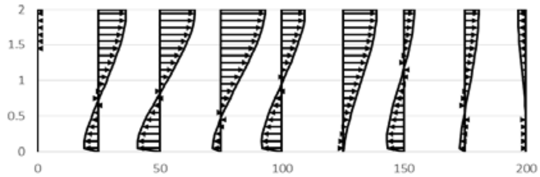

Fig. 15 Velocity vector on $\theta = 90^0$

The primary flow is the flow of water along the channel, and secondary flow is the flow of water perpendicular to its primary flow. It is shown in Fig. 13, water tends to flow to its curved direction and as the flow turns, shown in Fig. 14 and 15, water on the top layer tends to flow to another direction. This phenomenon caused erosion on the outer bank and deposition on the inner bank.

4.3 Pile on Curved Channel

Channel with 0.5m width, curved on two sections with 1.5m radius. The first section is curved 180^0 and other section 90^0. Circular pile with 5cm diameter placed on four positions, two in the straight section, and the rest on the curved section. Domain and model mesh can be seen in Fig. 16. Discharge of water flow is 9 L/s, with a depth of 6.5 cm. Initial bed sediment thickness is 20 cm.

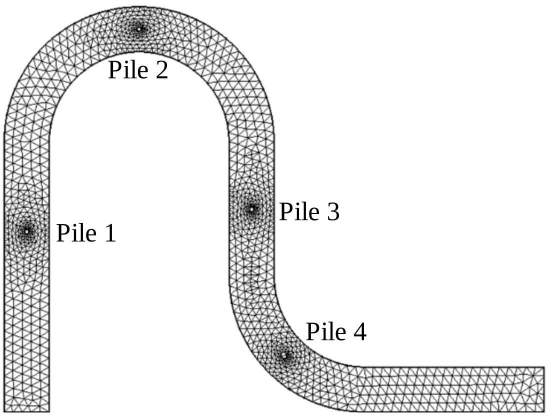

Fig. 16 The model domain of the pile around the curved channel

The simulation was conducted for 180 minutes with numerical Δt 0.0015 seconds and constant discharge. Simulation result shown here is time-series of scouring depth around pile as can be seen in Fig. 17.

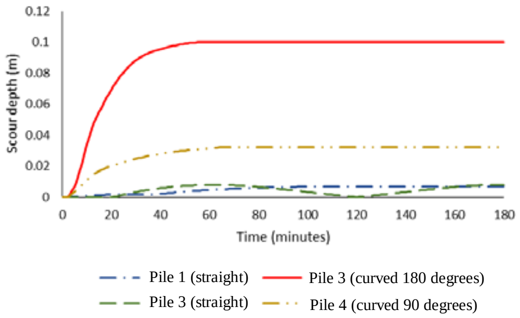

Fig. 17 Time-series of scour depth around pile on curved channel

The result shows that scouring is deeper in the curved section (Pile2 and Pile4) compared to those in the straight section. This is due to the addition of pile scouring and curved channel scouring, in that area local scouring also occurs due to channel bends. Also, degrees of curved channel contribute to scouring depth — a greater degree of curve results to deeper scouring.

5. CONCLUSIONS

FVCOM model successfully captured flow behavior around the pile and curved channel such as:

- Downflow upstream of the pile
- Wake vortex downstream of the pile
- Secondary flow on curved channel

The maximum value and time-series of scouring depth on a rectangular pile on the straight channel have very good accuracy compared to experimental studies. It is shown by Pearson correlation value of almost one and error percentage below 10 percent. On the curved channel case, the FVCOM model successfully captured the secondary flow phenomenon.

Pile and curved channel caused scouring in each case. Together, they make scouring phenomenon, even more, proven in FVCOM simulation which shows that scouring on piles on the curved channel is deeper than to those on straight one. The angle of the curve also has a positive correlation to scouring depth.

Study on the broader condition in scouring around pile on curved channel needs to be conducted in the future to enrich understanding of its particular problem. That condition could be mixed or cohesive sediment, a curved channel with a different angle, or real-world situation.

6. ACKNOWLEDGMENTS

This research is financially supported by the Institute for Research and Community Services of Institut Teknologi Bandung (LPPM-ITB) with its Research, Community Services, and Innovation Program (P3MI-ITB).

7. REFERENCES

[1] Munson B.R., Okiishi T.H., Huebsch W.W., Rothmayer A.P., Fundamentals of fluid mechanics 7th edition, John Wiley & Sons, Hoboken, 2002

[2] Annandale G.W., Scour technology mechanics and engineering practice, President Engineering and Hydrosystem Inc., McGraw-Hill, New York, 2006

[3] Versteeg H.K., Malalasekara W., An introduction to computational fluid dynamics, the finite volume method, second edition, Pearson, Harlow, 2007

[4] Mazumder S., Numerical methods for partial differential equations Academic Press, London, 2016

[5] Chen C., Liu H., Beardsley R.C., An unstructured, finite-volume, three-dimensional, primitive equation ocean model: application to coastal ocean and estuaries, J. of Atmospheric and Oceanic Technology, 20, 2003, pp.159-186

[6] Adikesuma T.N., Scouring around bridge pile on the curved river (laboratorium study) *(original: Gerusan sekitar pilar jembatan di tikungan sungai (kajian laboratorium))*, Master Program Thesis, Institut Teknologi Bandung, 2010

[7] Ameson L.A., Zevenbergen L.W., Lagasse P.F., Clopper P.E., Evaluating scour at bridges, 5th edition, Hydraulic Engineering Circular No. 18, Publication No. FHWA-HIF-12-003, Federal Highway Administration, Washington D.C., 2012

[8] Chen C., Beardsley R.C., Cowles G., Qi J., Lai Z., Gao G., Stuebe D., Liu H., Xu Q., Xue P., Ge J., Hu S., Ji R., Tian R., Huang H., Wu L., Lin H., Sun Y., Zhao L., An unstructured grid, finite-volume community ocean model FVCOM user manual, Department of Fisheries Oceanography, School for Marine Science and Technology, University of Massachusetts-Dartmouth, New Bedford, 2013

[9] Thanh N.V., Chung D.H., Nghien T.D., Prediction of the local scour at the square bridge pier using a 3D numerical model, Open J. of Appl. Sciences, 4, 2014, pp.34-42